The Yeast Vacuolar Membrane Proteome*[S]

Elena Wiederhold‡, Tejas Gandhi‡, Hjalmar P. Permentier‡, Rainer Breitling§, Bert Poolman‡, and Dirk J. Slotboom‡¶

Transport of solutes between the cytosol and the vacuolar lumen is of crucial importance for various functions of vacuoles, including ion homeostasis; detoxification; storage of different molecules such as amino acids, phosphate, and calcium ions; and proteolysis. To identify proteins that catalyze solute transport across the vacuolar membrane, the membrane proteome of purified *Saccharomyces cerevisiae* vacuoles was analyzed. Subtractive proteomics was used to distinguish contaminants from true vacuolar proteins by comparing the relative abundances of proteins in pure and crude preparations. A robust statistical analysis combining enrichment ranking with the double boundary iterative group analysis revealed that 148 proteins were significantly enriched in the pure vacuolar preparations. Among these proteins were well characterized vacuolar proteins, such as the subunits of the vacuolar H^+-ATPase, but also proteins that had not previously been assigned to a cellular location, many of which are likely novel vacuolar membrane transporters, *e.g.* for nucleosides and oligopeptides. Although the majority of contaminating proteins from other organelles were depleted from the pure vacuolar membranes, some proteins annotated to reside in other cellular locations were enriched along with the vacuolar proteins. In many cases the enrichment of these proteins is biologically relevant, and we discuss that a large group is involved in membrane fusion and protein trafficking to vacuoles and may have multiple localizations. Other proteins are degraded in vacuoles, and in some cases database annotations are likely to be incomplete or incorrect. Our work provides a wealth of information on vacuolar biology and a solid basis for further characterization of vacuolar functions. *Molecular & Cellular Proteomics 8:380–392, 2009.*

The vacuole is the largest organelle of yeast cells and the functional equivalent of the mammalian lysosome. The vacuole is surrounded by a single membrane, which contains the V-ATPase[1] complex that acidifies the interior of the vacuole. The pH difference of ~1.7 pH units between the vacuolar lumen and the cytosol is used as the driving force for substrate-proton antiport systems in the vacuolar membrane (1). Transport processes across the vacuolar membrane are important for many crucial functions of vacuoles: storage of organic molecules such as polyphosphates, mannans, and other carbohydrates (2, 3); detoxification, *i.e.* removal and accumulation of harmful substances such as heavy metals and drugs; and proton and ion homeostasis. Another major function of lysosomes and vacuoles is the intracellular proteolysis of cytosolic and membrane proteins (4, 5) and turnover of organelles, *e.g.* lipid bodies, mitochondria, peroxisomes, and portions of nuclei (6–9). Hydrolytic proteins in the lumen of vacuoles, including proteases, lipases, phosphatases, and nucleases, carry out these functions.

Whereas vacuolar luminal proteins have been studied fairly extensively (10, 11), our knowledge about the integral membrane proteins in the yeast vacuolar membrane is limited. A handful of vacuolar transport proteins have been identified and characterized by classical genetics and biochemical approaches (12–14). However, based on measurements of transport activities across the vacuolar membrane and determination of organic substance content in the vacuole lumen, the existence of many more proteins with translocation activities is expected. Transport systems for *S*-adenosylmethionine (15), purines (16), polyamines (17), and sulfate (18) have been postulated based on activity measurement, but the identity of the corresponding proteins has remained elusive.

Approximately 1000 yeast proteins (17–18% of the entire *Saccharomyces cerevisiae* proteome) do not have an annotated localization in the *Saccharomyces* Genome Database (SGD; release version June 9, 2007). It is likely that some of these are vacuolar. In recent years a couple of global protein localization studies (19–22) revealed the vacuolar localization of more than 40 putative proteins with unknown biological functions. However, these studies might have failed to detect

From the ‡Department of Biochemistry, Groningen Biomolecular Sciences and Biotechnology Institute and Zernike Institute for Advanced Materials, University of Groningen, Nijenborgh 4, 9747 AG Groningen, The Netherlands and §Groningen Bioinformatics Centre, University of Groningen, Kerklaan 30, 9751 NN Haren, The Netherlands

Received, August 8, 2008, and in revised form, October 14, 2008
Published, MCP Papers in Press, November 10, 2008, DOI 10.1074/mcp.M800372-MCP200

[1] The abbreviations used are: V-ATPase, vacuolar H^+-ATPase; ACTH, adrenocorticotropic hormone; AP, adaptor protein; CV, column volume; db-iGA, double boundary iterative group analysis; ER, endoplasmic reticulum; HOPS, homotypic fusion and vacuole protein sorting complex; iGA, iterative group analysis; iTRAQ, isobaric tag for relative and absolute quantitation; LOPIT, localization of organelle proteins by isotope tagging; MFS, major facilitator superfamily; PC, probability of change; RP, reverse-phase; SCX, strong cation exchange; SGD, *Saccharomyces* Genome Database; SNARE, soluble *N*-ethylmaleimide-sensitive factor attachment protein receptor complex; TEAB, triethylammonium bicarbonate; VPS, vacuolar protein sorting; GFP, green fluorescent protein; S/N, signal-to-noise; PMA1, plasma membrane ATPase 1; VTC, vacuolar transporter chaperone.

low abundance membrane proteins and possibly yielded incorrect information in some cases as the tags (such as the C-terminal GFP tag (19)) may affect targeting, resulting in the mislocalization of proteins.

To characterize the vacuolar membrane proteome and to identify novel vacuolar membrane proteins, we produced highly purified vacuolar membranes and analyzed their protein content by mass spectrometry. To discriminate between genuine vacuolar residents and contaminating proteins the subtractive proteomics technique localization of organelle proteins by isotope tagging (LOPIT) was used (23, 24) in conjunction with iTRAQ-based quantification. Analysis of the data by enrichment ranking and iterative group analysis (25) resulted in the identification of a group of 148 proteins that was enriched along with known vacuolar proteins in our preparation. In this group, 22 proteins without annotated localization could be assigned as likely to be vacuolar of which at least nine had confirmed or predicted translocation activity.

EXPERIMENTAL PROCEDURES

Yeast Strain and Cell Growth

Haploid *S. cerevisiae* W303 (MATα *ade2–1 leu2–3,112 his3–22,15 trp1–1 ura3–1 can1–100*) was used (26). All experiments were carried out as biological quadruplicates. For cell growth, 10 ml of YPD medium (0.3% yeast extract, 0.5% Bacto Peptone, 1% glucose) was inoculated with a colony from a fresh agar plate and incubated in a 100-ml Erlenmeyer flask for 15 h at 30 °C (shaking speed, 160 rpm). 50 ml of fresh YPD medium was inoculated with 0.5 ml of the preculture. Cells were grown for 6–8 h until the density was 1.5–2 $\times$ 10^7 cells/ml. At least four subsequent 200–500-fold dilutions in fresh medium followed by growth to a density of 1.5–2 $\times$ 10^7 cells/ml were carried out. Finally for large scale preparation, 12 liters of medium in a fermenter was inoculated with 20 ml of the last preculture. Cells were grown aerobically (30% oxygen saturation; stirring speed, 150 rpm) at a controlled pH of 6.3 in YPD medium. The doubling time was 1.5 h. Exponentially growing cells (1.5 $\times$ 10^7 cells/ml) were harvested by centrifugation at 4000 $\times$ g_{avg} for 5 min. Unless indicated otherwise, all steps were performed at room temperature. The cells were washed with 1 liter of double distilled water and centrifuged again. The wet weight of cells from a 12-liter culture was 20–30 g.

Isolation of Intact Vacuoles

Spheroplast formation was carried out according to Kipper *et al.* (27) with a few alterations. 20 g of cells was resuspended in 100 ml of 100 mM Tris-HCl, 10 mM DTT, pH 9.5, and incubated at 30 °C for 10 min while shaking at 50 rpm. Cells were centrifuged at 4000 $\times$ g_{avg} for 5 min, washed with 100 ml of water followed by a wash with 100 ml of 1.1 M sorbitol, and subsequently resuspended in 50 ml of 1.1 M sorbitol/20 g of cells. The cell wall was enzymatically digested with 1 ml of glusulase, which contained glucuronidase (90,000 units/ml) and sulfatase (19,000 units/ml) (catalog number NEE154001EA, PerkinElmer Life Sciences), 3 mg of zymolyase T20, and 3 mg of Glucanex (catalog number L1412, Sigma-Aldrich)/10 ml of suspension in the presence of 5 mM DTT. The suspension was incubated for 2.5 h at 30 °C while shaking at 60 rpm. In addition, the suspension was swirled manually every 15 min to ensure homogeneous digestion. Light microscopy was used to evaluate the extent of spheroplasts formation.

After digestion of the cell wall, the spheroplasts were cooled on ice. Each 25 ml of spheroplast suspension was pipetted on top of a layer of 25 ml of ice-cold solution containing 7.5% Ficoll and 1.1 M sorbitol in a centrifuge tube. The spheroplasts were washed through this Ficoll-sorbitol layer by centrifugation at 4,000 $\times$ g_{avg} for 20 min at 4 °C. The spheroplasts were lysed by 6$\times$ dilution of the spheroplast pellet with the ice-cold lysis buffer containing 10 mM Tris-MES, pH 6.9, 12% Ficoll, 0.1 mM $MgCl_2$ plus protease inhibitor mixture (catalog number 8215, Sigma-Aldrich). The suspension was homogenized on ice in a Dounce homogenizer (40 ml) by 15 strokes with a large clearance pestle "A" (catalog number 885300-0040, Kontes Glassware, Vineland, NJ). The cells and solutions were kept at 4 °C throughout.

For isolation of intact vacuoles, the protocol of Ohsumi and Anraku (28) was used with the following modifications. Samples of 20 ml of the spheroplast lysate were transferred to a centrifuge tube and overlaid with 10 ml of lysis buffer. Centrifugation was performed in a swing-out bucket rotor (Beckman, rotor type SW32Ti) at 20,000 rpm (50,000 $\times$ g_{avg}) for 30 min at 4 °C. The fraction floating on top of the tube contained the crude vacuoles, and it was collected and resuspended in 10 ml of lysis buffer/2–3 ml of crude vacuoles by homogenization with a loosely fitting Dounce homogenizer (5–6 strokes, pestle A). The homogenized crude vacuoles were overlaid in a centrifugation tube with a layer of 10 ml of 10 mM Tris-MES, pH 6.9, 8% Ficoll, 0.5 mM $MgCl_2$ plus proteinase inhibitor mixture and a second layer of 10 ml of the same buffer containing 4% Ficoll. Upon centrifugation at 20,000 rpm (50,000 $\times$ g_{avg}) for 45 min, intact vacuoles were floating on top of the 4% Ficoll solution as a white wafer. Purified vacuoles were collected with a spoon-shaped spatula prewetted in 4% Ficoll buffer.

Preparation of Vacuolar Membranes

The vacuoles, usually ~5 ml/20 g of cells, were lysed osmotically in the same volume of buffer consisting of 20 mM triethylammonium bicarbonate (TEAB), pH 8.0, 10 mM $MgCl_2$, 50 mM KCl and then diluted with 2 volumes of buffer containing 10 mM TEAB, pH 8.0, 5 mM $MgCl_2$, 25 mM KCl. Immediately (without incubation), the vacuolar membranes were recovered by centrifugation at 80,000 rpm (260,000 $\times$ g_{avg}) for 20 min (Beckman, rotor type TLA100.3). To remove peripheral proteins, the pellet was resuspended in 100 mM sodium carbonate, pH 11.8, and subsequently incubated in the same buffer plus 2 mM EDTA for 15 min on ice. The membranes were recovered by centrifugation for 60 min at 80,000 rpm (Beckman, TLA-100.3, 260,000 $\times$ g_{avg}). The protein concentration was determined by the BCA method (Pierce) after solubilization in 2% SDS.

Sample Preparation for Strong Cation Exchange (SCX)/RP LC and iTRAQ Labeling

For trypsinization, 100 μg of protein was resuspended in 30 μl of 500 mM TEAB, 33% methanol plus 0.05% SDS. Reduction of disulfide bonds with tris(2-carboxyethyl)phosphine hydrochloride (TCEP), cysteine modification with methyl methanethiosulfonate, digestion with trypsin (catalog number V511A, Promega), and iTRAQ labeling were performed according to the manufacturer's protocol (Applied Biosystems). For each biological replicate the peptides derived from proteins in the crude and pure vacuolar membrane preparations were labeled with two different iTRAQ reagents. For the first replicate iTRAQ reagents 114 (for the pure sample) and 116 (for the crude sample) were used, and for the second replicate reagents 115 (pure) and 117 (crude) were used. Then equal amounts of the four sets of labeled peptides from the two biological replicates were combined (see supplemental Table 1). For the third and fourth biological replicates a label swap was done: the iTRAQ reagents 114 and 115 were used for the crude samples, and reagents 116 and 117 were used for the pure samples. The two peptide mixtures (combined biological

replicates 1 and 2 and combined biological replicates 3 and 4) were subjected to chromatography and mass spectrometry analysis.

Prefractionation of Peptides by SCX

For off-line peptide prefractionation, a silica-based PolySULFOETHYL Aspartamide SCX column was used (catalog number 202SE0502, PolyLC Inc., Columbia, MD). The column was run at a flow rate of 200 μl/min on an Ettan MDLC (multidimensional liquid chromatography) system (Amersham Biosciences AB). Gradient solution A was 10 mM KH_2PO_4-H_3PO_4, pH 2.7, 25% ACN; gradient solution B was 10 mM KH_2PO_4-H_3PO_4, pH 2.7, 25% ACN, 1 M KCl. Gradient conditions were as follows: column equilibration with 5 column volumes (CVs) (1 CV = 0.7 ml) of 100% A. Peptides were loaded in 100% A, the column was washed with 5 CVs from 0 to 3% B, and peptides were eluted by 3–12% B in 12 CVs followed by 12–30% B in 3 CVs. Fractions were collected every 30 s in 96-well plates. Eluted peptides were concentrated to ~40 μl in a vacuum centrifuge and diluted 1:2 with 0.2% TFA. Depending on the complexity, either separate fractions or pools of two fractions were analyzed by RP LC MALDI-TOF/TOF.

RP LC and MALDI-TOF/TOF Analysis

Peptides were trapped on a precolumn (catalog number 5065-9914, Zorbax 300SB-C_{18}, Agilent Technologies, Santa Clara, CA) and then separated on a 75-μm × 150-mm analytical column (catalog number 5065-9911, Zorbax 300SB-C_{18}, Agilent Technologies) using the Ettan MDLC nano-LC system in the high throughput configuration (Amersham Biosciences AB). Gradient solution A contained 0.065% TFA, and gradient solution B contained 0.065% TFA, 84% ACN. Gradient conditions were as follows: equilibration of column, binding and washing of peptides was performed with 3% B, and elution was performed with 3–30% B in 60 min. The eluting peptides were mixed 1:4 with 2.2 mg/ml α-cyano-4-hydroxycinnamic acid matrix (LaserBio Labs, Sophia-Antipolis, France), 3 fmol/μl angiotensin II (Sigma-Aldrich), and 6 fmol/μl adrenocorticotropic hormone (ACTH) fragment 18–39 (Sigma-Aldrich) and spotted directly onto a MALDI target (200 spots) using a Probot system (LC Packings, Amsterdam, The Netherlands). Peptides were analyzed with a 4700 Proteomics analyzer (Applied Biosystems, Foster City, CA) MALDI-TOF/TOF mass spectrometer.

The MALDI-TOF/TOF instrument was operated in reflectron positive ionization mode in the *m/z* range 900–5000. The 30 most intense peaks above the signal-to-noise (S/N) threshold of 150 from each MS spectrum were selected for MS/MS fragmentation, and in addition the 10 most intense peaks in the S/N range of 150–30 were selected from the same MS spectrum. The MS/MS spectra were acquired using 1-kV acceleration voltage and air as collision gas at 5×10^{-7} torr. The precursor mass transmission window was set to ±5 Da. The peak lists of the acquired MS/MS spectra were generated using default settings and a S/N threshold of 10. The MS spectra were calibrated internally using angiotensin II (*m/z* = 1046.542) and ACTH 18–39 (*m/z* = 2465.199). MS/MS calibration of the instrument was performed daily using ACTH 18–39 fragment ions.

Database Search and Criteria for Protein Identification and Quantification

MS/MS peak lists were extracted by Global Proteome Server Explorer software, version 3.5 (Applied Biosystems) using default parameters and were automatically submitted to a database search. All MS/MS spectra were analyzed using Mascot (Matrix Science, London, UK; version 1.9.05) and X! Tandem (The Global Proteome Machine Organization; version 2006.04.01.2). Mascot and X! Tandem were set up to search a combined SGD assuming digestion by trypsin and allowing one or two missed cleavages for Mascot or X! Tandem, respectively. The database was created by combining forward and reversed entries of the SGD (release version June 9, 2007) and included sequences of porcine trypsin (NCBI accession number P00761) and human keratins (NCBI accession numbers P35908, P35527, P13645, and NP_006112) containing in total 13,443 protein entries. Mascot and X! Tandem were searched with a fragment ion mass tolerance of 0.20 Da and a parent ion tolerance of 200 ppm. Methyl methanethiosulfonate modification of cysteine and Applied Biosystems iTRAQ multiplexed quantitation chemistry of lysine and the N terminus were specified in Mascot and X! Tandem as fixed modifications. Deamidation of asparagine and glutamine, oxidation of methionine, and Applied Biosystems iTRAQ multiplexed quantitation chemistry of tyrosine were specified in Mascot and X! Tandem as variable modifications.

Scaffold (version Scaffold-01_06_17, Proteome Software Inc., Portland, OR) was used to validate MS/MS-based peptide and protein identifications. Peptide identifications were accepted if they could be established at greater than 95.0% probability as specified by the Peptide Prophet algorithm (29). Protein identifications were accepted if they could be established at greater than 99.0% probability and contained at least two uniquely identified peptides. Protein probabilities were assigned by the Protein Prophet algorithm (30). Proteins that contained similar peptides and could not be differentiated based on MS/MS analysis alone were grouped to satisfy the principle of parsimony. Those peptides were removed from the data set when quantification was performed. The false positive rate was calculated by dividing 2 times the number of proteins identified in the reversed database by 13,443, the sum of all proteins identified in forward and reversed versions of SGD. In two biological replicates, the false positive rate was 0.0035%, and in two other biological replicates no hits from the reversed database were detected using the criteria described above.

The relative quantification was based on peptides that were chemically labeled with isobaric reagents using the iTRAQ technique. The quantification information was obtained automatically by GPS Explorer software from the peak areas of the reporter ions (*m/z* 114.1, 115.1, 116.1, and 117.1 with a mass tolerance of 0.1 Da) from the MS/MS spectra. The peak areas were corrected for isotopic impurities by GPS Explorer using the information provided by the manufacturer in the certificate of analysis for each iTRAQ multiplex batch. Each protein quantification was based on two or four biological replicates, and if it was based on a single peptide only in one replicate, at least two identified peptides were necessary in one of the other biological replicates for a protein to be included in the analysis. Peptides that matched to multiple proteins were excluded from quantification, and indistinguishable isoforms of the same protein (*e.g.* ribosomal subunits A and B) were reported without the isoform specification. To select quantification data, those ratios were removed where the peak area of one reporter ion was below the signal-to-noise threshold of 10.

Statistical Analysis

Enrichment Ranking—Enrichment ranking was based on the rank products statistics (31), which was modified for use on peptide data as follows. If the same peptide was measured multiple times in the same biological sample, the iTRAQ ratios were averaged by calculating the mean. The peptide iTRAQ ratios were then listed in descending order, and the ranks were assigned so that the peptide with the highest ratio had rank 1, the peptide with the second highest ratio had rank 2, and so on. In this way, *peptide ranks* were obtained. The ranks of peptides derived from the same protein were averaged by calculating the median to minimize the effect of outliers, and the resulting

medians were then ranked again, resulting in *protein ranks* for each biological replicate. To combine the protein ranks of all replicates, the median of protein ranks across replicates was calculated and subsequently ranked again. This resulted in a single list of proteins with the most consistently enriched protein at the top (rank 1).

Iterative Group Analysis—To determine which proteins had co-enriched with known vacuolar proteins, a modified version of the iterative group analysis (iGA) algorithm (25) was applied. Proteins were assigned to one or several subcellular localizations, based on SGD annotations (release version June 9, 2007). "Cytosolic" and "cytoplasmic" localizations were combined as were "nucleus," "nucleolus," "nuclear membrane," and "nuclear pore." "Unknown" and unspecified "membrane" proteins were also combined in a single class. In the cases of multiple annotations (*e.g.* plasma membrane and vacuole), multiple classes were assigned and used for cluster analysis by iGA. For each localization class the list of enrichment-ranked proteins was analyzed using the hypergeometric statistics as described previously (31) using all possible windows to define groups. The window that showed the most surprising clustering of proteins from the same localization class, which is the highest probability of change ($-\log(PC)$) value as defined in Breitling *et al.* (31), was recorded. This procedure, which was called double boundary iGA, is more flexible than the original iGA approach, which only tests windows at the extremes (top or bottom) of the list and would for example miss clustering in the middle. Multiple testing-corrected p values were determined using 1000 random permutations of the protein list for each class. Corrected p values ≤ 0.005 were regarded as significant. A Mathematica implementation of the double boundary iGA method is provided as supplemental material.

RESULTS

Isolation of Vacuoles—For the proteomics analysis of yeast vacuolar membrane proteins, it was necessary to isolate vacuoles of a high purity. The protocol of Ohsumi and Anraku (28) was optimized and used in combination with the spheroplasting procedure from Kipper *et al.* (27). As detailed under "Experimental Procedures," we used two density centrifugation steps. In both steps the vacuoles floated to the top of the tube. The first centrifugation step yielded crude vacuoles, and after the second step we obtained highly pure vacuoles (Fig. 1).

The purity of the vacuoles was first evaluated using morphological criteria. The microscopic analysis revealed that vacuoles collected after the second density centrifugation step (Fig. 1*A*, *right-hand panel*) were highly pure compared with the crude organelles that were collected from the first centrifugation (Fig. 1*A*, *left-hand panel*, vacuoles are indicated by *arrows*). Next a qualitative impression of the enrichment and purity of the vacuoles was obtained by Western blot analysis using antibodies raised against specific organelle markers. As demonstrated in Fig. 1*B*, using the antibody against the vacuolar alkaline phosphatase PHO8, vacuoles were enriched on top of the centrifuge tube after the second density centrifugation. Plasma membrane contaminations were depleted from the final vacuolar fraction using the plasma membrane protein plasma membrane ATPase 1 (PMA1) as indicator. The mitochondrial outer membrane remained in the pellet of the first density centrifugation step and was also depleted from the final fraction as

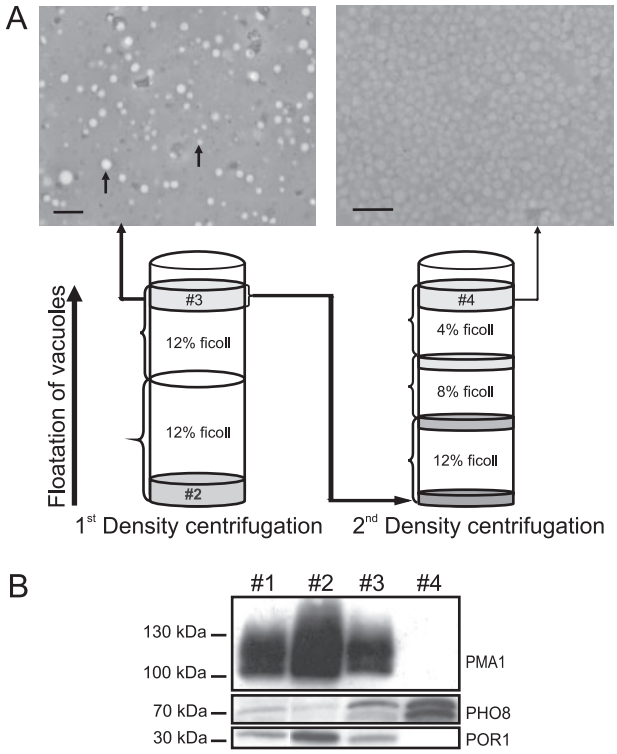

FIG. 1. **Isolation of vacuoles.** *A*, intact vacuoles were isolated according to Ohsumi and Anraku (28) using two steps of floatation density centrifugation. The crude vacuoles (indicated by *circles* in the *left-hand panel*) as collected from the top of the first density centrifugation were contaminated with other cellular constituents. Crude vacuoles were subjected to a second density centrifugation step. The highly pure vacuoles were collected from the top of the second density centrifugation (*right-hand panel*). *Bar*, 10 μm. *B*, the purity and the enrichment of the crude and pure vacuoles were assessed by means of Western blot analysis using antibodies raised against vacuolar alkaline phosphatase PHO8, plasma membrane ATPase PMA1, and mitochondrial outer membrane Porin-1 (*POR1*). Equal amounts of protein (20 μg, determined by the BCA assay) were loaded in each lane. *Lane 1*, total spheroplast lysate; *lane 2*, pellet after the first step of density centrifugation; *lane 3*, crude vacuoles obtained from the top of the first density centrifugation; *lane 4*, pure vacuoles obtained from the top of the second density centrifugation.

indicated by anti-Porin-1 antibodies. Thus, the final vacuolar preparation as obtained after two steps of density centrifugation was highly enriched in vacuoles and depleted of mitochondrial, late Golgi (not shown), and plasma membrane contaminations.

Subtractive Proteomics—Organelle preparations are never completely free of contaminants because of limitations in fractionation methods. To be able to distinguish vacuolar proteins from contaminants, we used the subtractive proteomics technique LOPIT. The idea of LOPIT is that the set of proteins that is physically associated with an organelle will co-enrich during the organelle isolation, whereas contaminants, although still present, will be depleted. We compared the relative abundances of proteins in the purified vacuoles (obtained after the second density centrifugation step; Fig. 1,

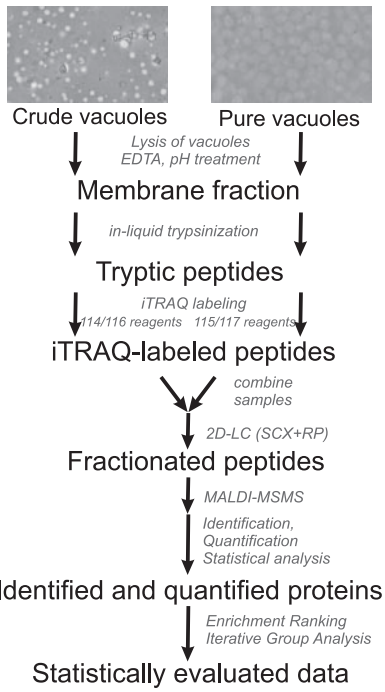

FIG. 2. **Work flow of LOPIT.** To compare relative abundances of proteins, the membranes of the crude vacuoles (Fig. 1, *#3*) and pure vacuoles (Fig. 1, *#4*) were stripped using EDTA and sodium carbonate at pH 11. The same amounts of protein from the stripped fractions 3 and 4 were digested with trypsin in the presence of 30% methanol (v/v). The tryptic peptides were labeled pairwise with different iTRAQ reagents, and the labeled peptides derived from the crude (114/116 reagents) and pure (115/117 reagents) vacuole membranes were combined. To reduce the complexity, the combined peptides were prefractionated by SCX, and each fraction was subjected to RP LC-MALDI analysis. The acquired spectra were analyzed by Mascot and X!Tandem. The identified and quantified peptides were ranked according to their iTRAQ ratios, and significant groups of enriched and depleted proteins were determined using double boundary iGA. *2D*, two-dimensional.

#4) and the crude vacuoles (obtained after the first density centrifugation step; Fig. 1, *#3*). The strategy is outlined in Fig. 2.

To facilitate the identification of low abundance vacuolar membrane proteins in the mass spectrometry analysis, vacuolar membranes were prepared in two steps to remove luminal and peripheral proteins. In the first step, vacuoles were lysed in the presence of EDTA, and vacuolar membranes were spun down by ultracentrifugation, and in the second step the membranes were stripped with sodium carbonate (pH 11.8).

In each of four biological replicates the relative protein abundances of the pure vacuolar membranes (from sample 4) and crude vacuolar membranes (from sample 3) were compared. The iTRAQ reagents were used to differentially label tryptic peptides derived from proteins in the crude and pure vacuolar membrane preparations (samples 3 and 4 in Fig. 1) as outlined in supplemental Table 1. Because four different iTRAQ labels were available (114/115/116/117) we could combine the pairs of labeled peptides from two different

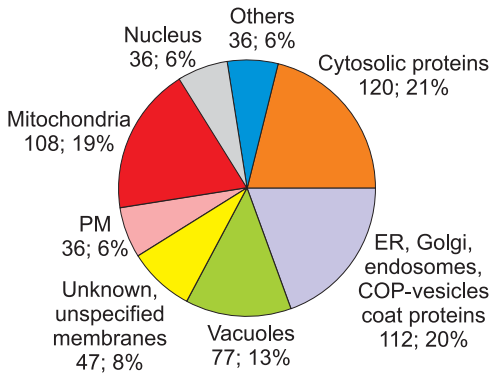

FIG. 3. **Annotated protein localizations of all identified and quantified proteins.** The entire data set contained 572 proteins and included both true vacuolar proteins and contaminants. The 77 identified vacuolar proteins cover 42% of all proteins annotated as vacuolar in SGD. *PM*, plasma membrane; *COP*, Coatomer Protein complex.

biological replicates for subsequent chromatographic separation and mass spectrometry analysis: peptides from crude vacuolar membranes were labeled with iTRAQ reagents 116 (replicate 1) or 117 (replicate 2), and those derived from the pure membranes were labeled with iTRAQ reagents 114 (replicate 1) or 115 (replicate 2). In a second mixture, the other two biological replicates were combined, and the labeling combinations were reversed, *i.e.* peptides from crude vacuolar membranes were labeled with iTRAQ reagents 114 (replicate 3) or 115 (replicate 4), and those from pure vacuolar membranes were labeled with 116 or 117. The labeled peptides mixtures were fractionated using cation exchange and reversed phase chromatography. Peptides were identified by MS/MS. The reporter peaks of the iTRAQ reagents in the MS/MS spectra were used for quantification. The reporter peak area of a peptide derived from proteins present in the *pure* vacuolar membranes was divided by the reporter peak area of the peptide derived from proteins in the *crude* membranes, resulting in an iTRAQ ratio. So in theory, peptides with ratios larger than 1 were enriched in the pure vacuolar membrane fraction, and conversely, ratios smaller than 1 indicated depletion (peptides derived from contaminant proteins).

572 proteins were identified and quantified (supplemental Table 3) of which 484 (84%) were found in both mass spectrometry analyses. Because only those peptides were quantified for which all iTRAQ reporter fragments (114/115/116/117) were detected, the 484 proteins had been present in all four biological replicates, and the remaining 88 proteins had been present in at least two biological replicates, indicating a high reproducibility of the procedure. As expected, the identified proteins were derived from various cellular locations because a mixture of highly pure and crude vacuolar membranes (containing contaminants) was analyzed (Fig. 3). Almost 60% of the 572 identified proteins belonged to three major groups: cytosolic proteins, mitochondrial proteins, and components of the protein trafficking machinery including ER,

Golgi, Coatomer Protein complex (COP) coat proteins, and the endosome. More than 63% (363 proteins) of the identified proteins did not contain predicted transmembrane domains. In the entire data set, 77 proteins were annotated as "vacuolar" in SGD, representing ~42% of the total number of proteins annotated as vacuolar. The remaining 58% of annotated vacuolar proteins were not found, and reasons for their absence will be discussed below. Intriguingly 47 proteins of the 572 proteins identified in our analysis did not have a known localization. Such proteins with unknown localizations are candidate novel vacuolar (membrane) proteins.

Enrichment Ranking and Iterative Group Analysis—In theory, each protein with an absolute iTRAQ ratio larger than 1 could be considered enriched in the pure vacuolar preparation. In practice, however, experimental errors prior to the mixing of the peptides, such as those associated with protein concentration determination or incomplete digestion or labeling, interfere with such direct assignment. To reliably determine which of the identified proteins were enriched in the purified vacuolar fraction, enrichment ranking (31) in conjunction with iGA (25) was applied.

A list of all identified proteins was made, ranked in the order of descending iTRAQ ratios. To this end, the data from multiple peptides per protein and multiple biological replicates were analyzed in a robust way as described in detail under "Experimental Procedures.". We then used a statistical test, based on iGA (25), to determine whether proteins from particular subcellular localizations as annotated in the SGD were significantly clustered in the list. iGA was originally developed for the functional annotation of microarray results and is based on hypergeometric statistics. It is applicable to small and noisy data sets with a relatively low number of replicates. A major advantage for the analysis is the robustness of iGA against imperfect assignments of the functional classes, in our case incorrect or incomplete annotation of the localization of proteins in the SGD. To make iGA applicable to our purposes, we modified the original algorithm as described under "Experimental Procedure," resulting in the so-called double boundary iGA (db-iGA) approach. We applied the double boundary iGA to the set of 572 proteins that were ranked as described above.

As expected, known vacuolar proteins were clustered among the proteins with the highest iTRAQ ratios, *i.e.* the proteins that were most enriched in the density centrifugation. The iGA defined a group of 148 proteins at the top of the ranked list in which most annotated vacuolar proteins were clustered (PC value of 3.4×10^{-37}; multiple testing-corrected p value <0.001). This group was named the enriched cluster and contained 69 proteins annotated as vacuolar, 22 proteins with no known localization, and 57 proteins annotated as localized to other organelles (Fig. 5*A*). The latter were mainly from the ER-Golgi-endosome network, cytosol, and plasma membrane. These proteins, which are co-enriched with the vacuolar proteins, may represent proteins targeted to the vacuoles for degradation, proteins with multiple localizations, or proteins with incomplete or incorrect database annotation, and they will be discussed below. The 22 proteins with no known localization represent potential novel vacuolar proteins (Table I). As mentioned above, in the entire data set we could identify 77 proteins annotated as vacuolar. The iGA analysis excluded eight of these proteins from the enriched vacuolar cluster. Possible reasons for the exclusion will be discussed below.

Non-vacuolar proteins, such as those from mitochondria, were expected to be depleted as indicated by Western blot analysis (Fig. 1*B*). The double boundary iGA was used to test whether proteins with different annotated localizations were significantly clustered in the ranked list. The ranges, PC values, and corrected p values for each cluster are summarized in supplemental Table 2. The group containing mitochondrial proteins was well defined at the bottom of the list and was regarded as strongly depleted from the pure vacuolar fraction (Fig. 4). The group of endosomal proteins was found to be significantly clustered, but it was overlapping with the cluster of enriched vacuolar proteins (Fig. 4). The overlap suggested that some of the proteins were co-enriched with the vacuolar proteins and might represent proteins targeted to vacuoles for degradation or, more likely, proteins with multiple localizations as will be discussed below. Proteins with other annotated localization (ER, Golgi, plasma membrane, nucleus, or cytosol) did not form significant clusters.

DISCUSSION

Proteins with Annotated Vacuolar Localization

Enriched Vacuolar Proteins—69 proteins in the enriched group were annotated as vacuolar in the SGD, most of which are well characterized vacuolar residents (Fig. 5*A*). Their vacuolar localizations are well established, justifying the use of the annotations in iterative group analyses. These vacuolar proteins include eight subunits of the vacuole V-type ATPase (A, C, D, H, E, a, d, and e) and canonical vacuolar proteases and phosphatases such as APE3, PRB1, CPS1, DAP2, and PHO8 (*cf.* alkaline phosphatase in Fig. 1*B*) as well as putative hydrolases ECM14, YBR139W, YNL115C, and YNL217W.

The largest functional group of enriched vacuolar proteins contains 27 proteins with confirmed or predicted transport activity (Fig. 5). Among them are 18 well characterized vacuolar transport proteins, such as the glutathione *S*-conjugate transporter YCF1, the zinc transporter ZRC1, and neutral amino acid transporters AVT1 and AVT3. Interestingly we also detected AVT7, which is related to AVT1/3. Whereas the substrate specificity and the vacuolar localization of AVT1 and AVT3 were unambiguously demonstrated by immunofluorescence and transport activity measurements (14), AVT7 localization was ambiguous as it was found at the plasma membrane (14) or at the ER as GFP-tagged protein (19). Our results clearly demonstrate a high enrichment of AVT7 in the vacuole.

TABLE I

Novel vacuolar proteins

22 proteins without known localizations were determined as enriched along with pure vacuolar membranes (Fig. 5). Nine proteins are predicted transporters, and 13 display versatile functions. NSF, *N*-ethylmaleimide-sensitive factor; ABC, ATP-binding cassette. RSN, Restin; DHHC, denote amino acids (Asp-His-His-Cys); TMHMM, Trans Membrane Hidden Markov Model.

Protein accession numbers	Protein name	TMHMM[a]	Function (predicted)[b]	Localization[b]	GFP localization
Transport proteins					
YAL022C	FUN26	11	Nucleoside transporter	Membrane	No
YBR235W	YBR235W	10	Cation/chloride co-transporter	Unknown	Ambiguous
YCR011C	ADP1	7	ABC transporter	Membrane	ER
YDL054C	MCH1	11	MFS transporter	Membrane	Vacuolar membrane
YGL114W	YGL114W	12	Oligopeptide transporter	Membrane	No
YJR124C	YJR124C	9	MFS transporter	Unknown	No
YKL064W	MNR2	2	Magnesium and cobalt ion transporter	Membrane	Ambiguous
YLR047C	FRE8	5	Ferric reductase-like transmembrane component	Membrane	No
YOR291W	YOR291W	11	Cation transporter ATPase	Membrane	ER
Other functions					
YAR028W	YAR028W	2	Unknown	Unknown	Ambiguous
YBL050W	SEC17	0	Soluble NSF attachment protein (SNAP) involved in ER to Golgi transport	Unknown	No
YBR074W	YBR074W	8	Metalloendopeptidase	Unknown	No
YDR089W	YDR089W	3	Protein involved in membrane organization and biogenesis	Unknown	Ambiguous
YGR141W	VPS62	0	Protein involved in protein targeting to vacuole	Unknown	No
YLR173W	YLR173W	1	Unknown	Unknown	No
YLR240W	VPS34	0	Protein kinase	Unknown	Punctate, endosome
YLR241W	YLR241W	11	RSN (yeast)-related membrane protein	Unknown	No
YLR360W	VPS38	0	Protein involved in late endosome to vacuole transport	Unknown	Endosome
YMR266W	RSN1	11	Protein involved in Golgi to plasma membrane trafficking	Unknown	Cell periphery
YOR034C	AKR2	7	Zinc finger DHHC domain-containing protein involved in endocytosis	Unknown	No
YPL057C	SUR1	2	Mannosyltransferase involved in sphingolipid biosynthesis (70)	Intracellular	Vacuolar lumen
YPL120W	VPS30	0	Protein involved in targeting to vacuole and autophagy	Membrane	Vacuolar lumen

[a] Displays the number of transmembrane domains corrected for N-terminal signal peptide. From the number of transmembrane helices predicted by TMHMM, the first transmembrane domain was subtracted if it overlapped with the signal peptide as predicted by SignalP.

[b] Information was obtained from SGD.

The enriched proteins included 10 proteins annotated not only as vacuolar but also bearing annotations for other subcellular localizations such as cytosol, mitochondria, endosome, and plasma membrane (Fig. 5*A*). A literature survey confirmed the vacuolar function of all 10 proteins, and interestingly all of them are involved in membrane fusion either directly, *e.g.* as members of the homotypic fusion and vacuole protein sorting (HOPS) complex, or indirectly by transmitting signals. Proteins involved in membrane fusion, trafficking, and targeting to the vacuole constitute the second largest functional group in the group of enriched proteins. They will be discussed in detail below.

Depleted Vacuolar Proteins—The 424 depleted proteins should be regarded as non-vacuolar proteins (contaminants) and include for instance all 35 detected ribosomal proteins, the plasma membrane ATPase, and the mitochondrial porin (*cf*. PMA1 and POR1 in Fig. 1*B*). However, this group also contained eight proteins that were previously annotated as vacuolar. Among them, there are four well characterized vacuolar proteins (VTC2, VTC3, VMA2, and PEP4). VTC proteins belong to the vacuolar transporter chaperones, which are found at the ER and vacuole (32). Upon induction of autophagy under nutrient-limiting conditions, the VTC complex is recruited to vacuoles and concentrated at autophagic tubes of the membrane (32). Interestingly whereas VTC2 and VTC3 were depleted in our analysis, two other members of the vacuolar transporter chaperones, VTC1 and VTC4, were specifically enriched in the pure vacuolar membrane fraction suggesting distinct biological functions. The soluble subunit B (VMA2) of V-ATPase is loosely attached and may easily be lost during sample preparation (33), which could explain its apparent depletion. The reason why PEP4 is depleted is not

FIG. 4. **Enrichment clusters of proteins of different annotated localizations.** All 572 identified proteins were ranked according to their iTRAQ ratios, and db-iGA was applied to determine significant clusters of proteins with the same localization. The most enriched proteins are depicted at the *top* of the figure. Each *horizontal bar* in the *column* on the *right* represents a single protein colored according to the annotated subcellular localizations of a protein: *green*, vacuole; *pink*, plasma membrane; *purple*, ER, Golgi, and endosome; *orange*, cytosol and cytoplasm; *red*, mitochondrial; *gray*, nucleus; *yellow*, unknown; and *blue*, others. The *vertical bars* indicate the range that shows a significant cluster of proteins from a particular subcellular localization as determined by db-iGA: *green*, vacuolar proteins, rank 1–148; *light purple*, endosome, rank 88–214; *red*, mitochondrion, rank 326–570. The clustering of ER, Golgi nuclear, cytosolic, and plasma membrane proteins was not significant.

clear. However, it has been shown that PEP4 is secreted (instead of targeted to the vacuole) upon overexpression (34), and the protein has also been found in highly purified mitochondria, indicating that the vacuole may not be the only or predominant destination of PEP4.

Four proteins (GRX7, SSA2, YKT6, and YKL077W) with shared localization in vacuoles and another organelle were depleted in our experiment. It is very well possible that GRX7 indeed is not a vacuolar protein as a recent publication demonstrated a *cis*-Golgi localization of GRX7 (YBR014C), and its function is to catalyze glutathione-dependent reduction of disulfide bonds in oxidative stress conditions (35). SSA2 is a member of the heat shock protein 70 family and contributes to the transport of the vacuolar aminopeptidase APE1 and the cytosolic fructose-1,6-bisphosphatase FBP1 from the cytosol to the vacuole (36, 37). We could detect neither APE1 nor FBP1 in our vacuolar preparations possibly because SSA2 was present at a different subcellular location, *e.g.* acting as chaperone in folding of newly synthesized cytosolic enzymes (38). YKT6 is a protein with acyltransferase activity, which is required for multiple protein targeting pathways to the vacuole (39) participating in the *cis*-multi-SNARE (soluble *N*-ethylmaleimide-sensitive factor attachment protein receptor) complex (40). This pathway includes the ER where YKT6 is involved in ER to Golgi transport (41), endosomes where it is implicated in transport from Golgi to endosomes (42), and the vacuole where it plays a role in homotypic fusion (40). We could not identify any other components of the *cis*-multi-SNARE complex (VAM3, VAM7, or NYV1) except for the vesicle SNARE protein VTI1, which was also depleted in our analysis. This indicates that the *cis*-multi-SNARE complex was not located at the vacuolar membranes in our experiments. Finally we could not confirm vacuolar localization of YKL077W, which was previously assigned to the vacuolar lumen based on a high throughput localization study using GFP fusions (19), and we suggest that it represents an incorrect annotation.

Undetected Vacuolar Proteins—In total we found 77 proteins that were annotated as vacuolar in the SGD. This covers 42% of all proteins annotated as vacuolar in the database. There are many possible reasons for not finding a large portion of proteins that were annotated as vacuolar. First, there is a group of proteins that have limited accessibility for digestion

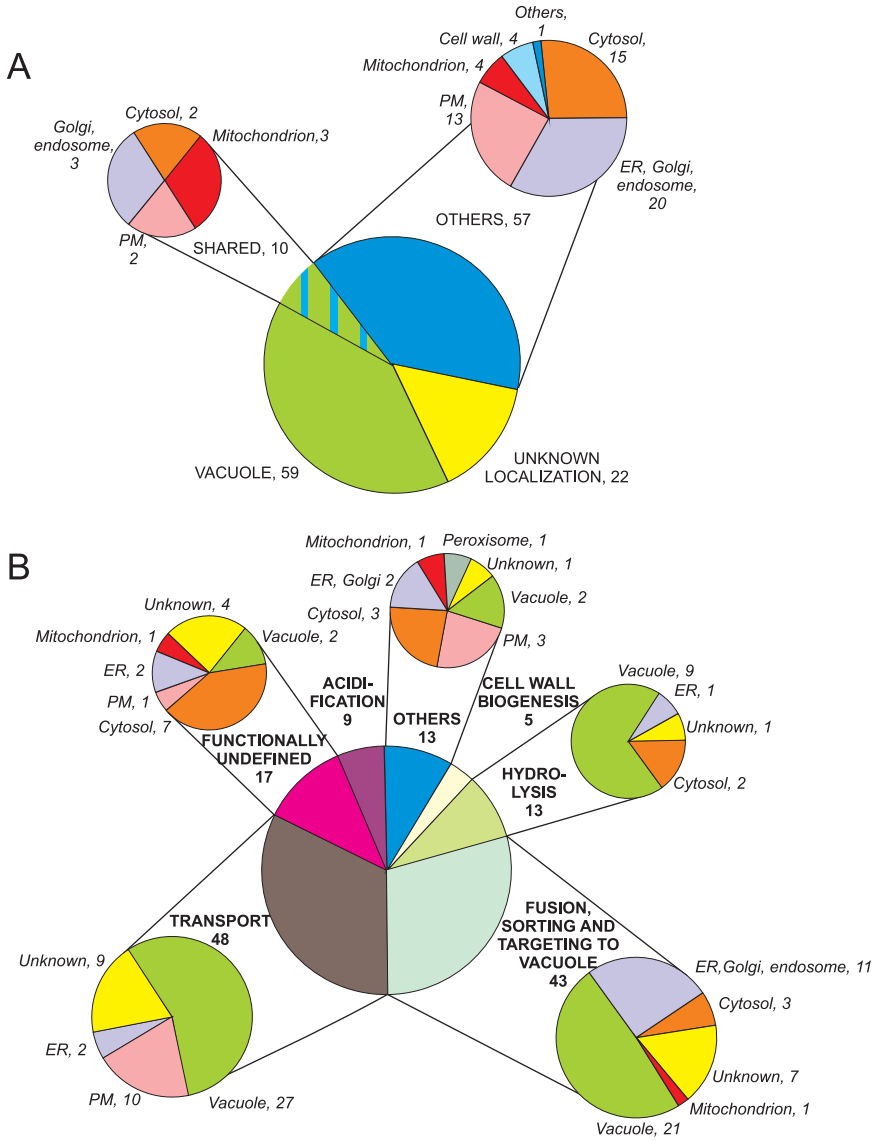

FIG. 5. **Grouping of enriched proteins.** *A*, annotated localizations of enriched proteins. Db-iGA showed that 148 proteins were enriched together with known vacuolar proteins. 69 of these proteins had been assigned previously to the vacuole, including 10 proteins with multiple localizations. Of the remaining proteins, 57 proteins had been annotated previously to organelles other than the vacuole. *Colors* are as in Fig. 4. *B*, annotated functional categories of enriched proteins. The major functional group among the 148 enriched proteins represented 48 proteins that were known or were predicted to be involved in transport processes. 27 proteins from this group (54%) were known to be vacuolar. 22 novel vacuolar proteins were distributed among the various functional groups (*yellow segments*). *PM*, plasma membrane.

or identification by LC-MALDI because of their high hydrophobicity or small size, *e.g.* subunits c, c′, and c″ of V-ATPase. Second, some proteins are of low abundance or may not be expressed under our experimental conditions. For instance, the vacuolar zinc transporter ZRT3 is expressed under zinc-limiting conditions (43). As yeast was grown on rich complete medium, it is unlikely that elements such as zinc ions were limiting for growth. Therefore we assume that ZRT3 (among others) was not expressed to a sufficiently high level for detection. Third, because we aimed at the identification of membrane proteins, we stripped peripheral proteins from the vacuolar membranes using EDTA and high pH treatments. Many peripheral proteins, such as components of regulator of the ATPase of vacuolar and endosomal membranes (RAVE), SNARE, and CCZ1-MON1 complexes, involved in vacuole biogenesis, homotypic vacuole fusion, and protein targeting to the vacuole may have been lost during sample preparation. Fourth, a number of database annotations are based solely on GFP tagging studies, which could create localization artifacts. In those cases previous assignments as vacuolar may have been incorrect.

Enriched Proteins with Other or Unknown Annotated Localization

A group of 57 proteins with database annotations for various non-vacuolar localizations was enriched along with the known vacuolar proteins. It contained proteins of the ER, Golgi apparatus, endosomes, cytosol, plasma membrane, mitochondrion, and cell wall (Fig. 5*A*). The group of proteins with localizations other than the vacuole might be true vacuolar proteins with incomplete or incorrect annotation. For example, the putative protease YBR074W has no database annotation for localization but is clearly enriched and is most likely

a true vacuolar proteolytic enzyme. Similarly STV1, an isoform of VPH1 (subunit a of V-ATPase), was enriched in the pure vacuole fraction. STV1 has been reported to be localized mainly in the Golgi and endosomes, but our analysis shows that STV1 is also vacuolar. The two largest functional groups of enriched proteins without vacuolar database annotations are proteins involved in membrane fusion, trafficking, and targeting to vacuoles and transport proteins.

Proteins Involved in Membrane Fusion, Protein Sorting, and Targeting to Vacuoles—A group of 43 enriched proteins is involved in homotypic fusion of vacuole membranes, protein trafficking, and targeting to the vacuole (Fig. 5*B*). This group included subunits of the SNARE complex and the HOPS complex (of the latter, all six subunits, PEP3, PEP5, VPS16, VPS33, VPS41, and VAM6, were enriched), proteins of the vacuolar protein sorting (VPS) family, and subunits of the clathrin adaptor protein (AP) complex. Nine proteins in this functional group have annotated localizations for ER, Golgi, or endosome. However, these proteins are likely to be true vacuolar proteins possibly with multiple localizations.

It is important to stress that most proteins with annotated ER, Golgi, and endosomal localization were not enriched in our analysis, indicating that we did not enrich the entire organelles along with the vacuoles but that instead a few proteins only annotated as ER, Golgi, or endosome have an (additional) vacuolar localization. For instance, all detected mannosyltransferases of the Golgi apparatus were depleted. Also the component VPS8 of the C-core vacuole/endosome tethering complex, specifically associated with *endosomal* vesicle fusion, was depleted, whereas the other four subunits that are shared with the HOPS complex of *vacuolar* membrane fusion (PEP3, PEP5, VPS16, and VPS33) were enriched. Membrane tethering and fusion are regulated by Rab-GTPases (for a review, see Ref. 44). The vacuolar HOPS and the endosomal C-core vacuole/endosome tethering complex specifically associate with two different Rab-GTPases, YPT7 (45) and VPS21 (40), respectively. Whereas YPT7 was enriched in our experiment, VPS21 was depleted, indicating that proteins with unique endosome/Golgi localization were not enriched in our analysis.

The group of enriched proteins also contained components of the protein kinase complexes TORC1 and TORC2 (for a review see, Ref. 46). TORC1 contains among others TOR1 or TOR2 (phosphatidylinositol kinase-related protein kinases) and KOG1 (which might act as scaffold protein) and regulates cell growth in response to nutrient availability (47), but it is also known to play a role in regulation of amino acid synthesis (47), endocytosis, and protein trafficking to the vacuole (48, 49). Different components of TORC1 and TORC2 were previously found at the plasma membrane and membranes of unknown cellular origin (50), at the endosomal and Golgi membrane (47), and at the mitochondrion (51). We show that a population of TOR1, TOR2, and KOG1 is associated with the vacuolar membrane where it might modulate vacuolar morphology and segregation (52).

Another protein linked to membrane fusion is NCR1, which is a known vacuolar membrane protein. NCR1 displays sphingolipid transport activity and is an orthologue of the human Niemann-Pick C1 protein (53). The intracellular trafficking of NCR1 and targeting to the vacuole were demonstrated to be dependent on the AP-3 complex (54), two subunits of which (APL5 and APM3) are annotated as Golgi or Golgi/endosome but were found enriched in our analysis and are (also) vacuolar proteins.

Five proteins from the functional group of fusion, trafficking, and targeting to vacuoles (VPS30, VPS62, RSN1, SEC17, and AKR2) were not previously assigned to any organelle, and we report their vacuolar localization. The involvement of SEC17 in dissociation and association of vacuolar SNARE complexes together with the HOPS complex has been reported (55).

YPT7 and YMR221C were previously assigned to the mitochondrial membrane based on high throughput analysis of yeast mitochondria (51, 56, 57) as well as to the vacuolar membrane (58). YPT7 is involved in endocytosis (59), and YMR221C does not have a known function. Although the latter was detected in the mitochondrial proteome, our analysis indicates that it specifically localizes to the vacuole under our experimental conditions. A vacuolar localization of YMR221C is consistent with a possible function in autophagy based on its physical interaction with ATG27 (60), which was also enriched in our analysis.

We found two cytosolic membrane fusion-related proteins, ENO2 and VAC7, to be enriched in the vacuolar fraction. ENO2, which is an essential glycolytic enzyme (enolase), was previously shown together with its isoform ENO1 to activate homotypic vacuolar fusion and protein transport to the vacuole (61). Also VAC7, which links phosphatidylinositol 3-phosphate 5-kinase signaling to vacuole morphology (62) by activating the FAB1 kinase activity, was shown previously to display multiple subcellular locations, vacuolar (63) and cytosolic (22). The phosphatidylinositol 3-phosphate 5-kinase FAB1 itself was also enriched, has multiple annotated localizations (mitochondrion, endosome, and vacuole), and is involved in vacuolar sorting and homeostasis (64, 65).

Transport Proteins—The largest functional group of enriched proteins contains 48 proteins with predicted or confirmed transport activity, approximately half of which (27 proteins) had been assigned a vacuolar localization before (Fig. 5). Two putative membrane transport proteins, YBR287W and YPR003C, that were previously annotated as ER residents based on the global protein localization study (19), were found to be vacuolar in our proteomics analysis (Fig. 5*B*). It is likely that these proteins have in fact a vacuolar localization but were previously misannotated as ER residents because the GFP tag affected their correct localization. Similarly several well known vacuolar transporters such as AVT1, VCX1, and PHO91 could not reach their destination at the vacuolar membrane when GFP was fused to their C termini and were trapped in the ER. Also these proteins are in the list of enriched vacuolar proteins.

We identified 22 proteins (Table I and Fig. 5) that were not previously assigned to any location, and here we report their vacuolar localization for the first time. Among these novel vacuolar proteins there are nine predicted transporters and several other integral membrane proteins that might also have transport function. The putative transporters include an ATP-binding cassette transporter (ADP1), a P-type ATPase (YOR291), and several secondary active transporters. Interestingly among the nine predicted transporters is a known nucleoside transporter (FUN26 (YAL022C) (66)) and a putative oligopeptide transporter of the oligopeptide transporter family (YGL114W). As the vacuole is the center of catabolic processes, these proteins are candidates to recycle the products of degradation back to the cytosol.

Proteins Degraded in Vacuoles—Degraded proteins are physically present in vacuoles and therefore are not contaminations. As we used subtractive proteomics to compare the vacuolar membrane proteome from two preparations (crude and pure vacuoles; Fig. 2) that were both already devoid of the bulk of other cellular constituents, it was not possible to discriminate between proteins that are degraded in the vacuole and true residents that function in the vacuole. The reason why we did not use even cruder fractions to compare with the pure vacuoles is that the number and amounts of added contaminants would increase dramatically, making the detection and identification of low abundance vacuolar proteins more difficult. 13 enriched proteins are well characterized plasma membrane proteins (Fig. 5), including 10 known plasma membrane transporters presumably because they are targeted to the vacuole for degradation. Plasma membrane proteins are known to be degraded in the vacuole (*e.g.* the general amino acid transporter GAP1 (67)), and our analysis indicates that we also enriched for plasma membrane proteins targeted to the vacuole for proteolysis. This result is in agreement with the GPF fusion analysis showing fluorescent signals at both the vacuolar lumen and the plasma membrane. Five enriched proteins were from the cell wall biogenesis pathway and annotated as cell wall and bud neck proteins. Although only the bud neck protein CHS2 is known to be degraded in the vacuole (68), our analysis indicates that the other four, BGL2, YJL171C, GAS1, and FKS1, are also targeted to the vacuole for degradation. This assumption is supported by the GFP localization study as BGL2 and FKS1 do localize to the vacuolar lumen when fused with GFP, although the vacuolar localization of BGL2 as a GFP fusion was interpreted as mislocalization.

The notion that proteins targeted to vacuoles for degradation are enriched in our analysis shows that some care must be taken when interpreting the list of enriched proteins. To illustrate this point, the group with annotated vacuolar localization included nine predicted but uncharacterized transporters (19, 69). Six of them have confirmed vacuolar *membrane* localizations: three members of the major facilitator superfamily (MFS) (YCR023C YBR241C and YDR119W), two proteins with predicted cystinosine/ERS1 repeats (YOL092W and YDR352W), and MAM3, which might play a role in cellular manganese ion homeostasis. Our analysis indicates that these transporters indeed represent true vacuolar transporters. Three other putative transporters, YGR125W (predicted sulfate transporter), YMR221C (MFS), and FRE6 (ferric reductase), had been reported as localizing to the vacuolar *lumen* as GFP fusions (19) and might be vacuolar transporters or proteins targeted to vacuoles for degradation.

Conclusion

To find previously undetected vacuolar membrane proteins, we performed a proteomics analysis on highly purified vacuoles. To deal with the problem of contaminants we used LOPIT (23). We performed rigorous statistical analyses to determine the cluster of proteins enriched with vacuoles as well as clusters of depleted proteins from different locations. Our analysis yields insight in the dynamics of the vacuolar proteome (illustrated by proteins with multiple localizations) and in the function of vacuoles (degradation of proteins and novel putative transporters). We also found several proteins with erroneous localization annotations. Our work provides a solid basis for further characterization of vacuolar functions.

Acknowledgments—We thank Albert Sickmann, Fabrizia Fusetti, and Liesbeth Veenhoff for advice and helpful discussions in various stages of the project. We also thank L. Veenhoff for critically reading the manuscript.

* The work was supported by The Netherlands Proteomics Centre, The Netherlands Organisation for Scientific Research (NWO, vidi grant (to D. J. S.)), and the BioRange program of the Netherlands Bioinformatics Centre, which is supported by a Besluit subsidies investeringen kennisinfrastructuur (BSIK) grant through the Netherlands Genomics Initiative. The costs of publication of this article were defrayed in part by the payment of page charges. This article must therefore be hereby marked "*advertisement*" in accordance with 18 U.S.C. Section 1734 solely to indicate this fact.

S The on-line version of this article (available at http://www.mcponline.org) contains supplemental material.

¶ To whom correspondence should be addressed. E-mail: d.j.slotboom@rug.nl.

REFERENCES

1. Kakinuma, Y., Ohsumi, Y., and Anraku, Y. (1981) Properties of H^+-translocating adenosine triphosphatase in vacuolar membranes of *Saccharomyces cerevisiae*. *J. Biol. Chem.* **256,** 10859–10863
2. Shirahama, K., Yazaki, Y., Sakano, K., Wada, Y., and Ohsumi, Y. (1996) Vacuolar function in the phosphate homeostasis of the yeast *Saccharomyces cerevisiae*. *Plant Cell Physiol.* **37,** 1090–1093
3. Indge, K. J. (1968) Polyphosphates of the yeast cell vacuole. *J. Gen. Microbiol.* **51,** 447–455
4. Horst, M., Knecht, E. C., and Schu, P. V. (1999) Import into and degradation of cytosolic proteins by isolated yeast vacuoles. *Mol. Biol. Cell* **10,** 2879–2889
5. Rotin, D., Staub, O., and Haguenauer-Tsapis, R. (2000) Ubiquitination and endocytosis of plasma membrane proteins: role of NEDD4/RSP5p family of ubiquitin-protein ligases. *J. Membr. Biol.* **176,** 1–17
6. Moeller, C. H., and Thomson, W. W. (1979) Uptake of lipid bodies by the yeast vacuole involving areas of the tonoplast depleted of intramembranous particles. *J. Ultrastruct. Res.* **68,** 38–45

7. Kim, I., Rodriguez-Enriquez, S., and Lemasters, J. J. (2007) Selective degradation of mitochondria by mitophagy. *Arch. Biochem. Biophys.* **462,** 245–253
8. Sakai, Y., Koller, A., Rangell, L. K., Keller, G. A., and Subramani, S. (1998) Peroxisome degradation by microautophagy in *Pichia pastoris*: identification of specific steps and morphological intermediates. *J. Cell Biol.* **141,** 625–636
9. Roberts, P., Moshitch-Moshkovitz, S., Kvam, E., O'Toole, E., Winey, M., and Goldfarb, D. S. (2003) Piecemeal microautophagy of nucleus in *Saccharomyces cerevisiae*. *Mol. Biol. Cell* **14,** 129–141
10. Wiemken, A., Schellenberg, M., and Urech, K. (1979) Vacuoles: the sole compartments of digestive enzymes in yeast (*Saccharomyces cerevisiae*)? *Arch. Microbiol.* **123,** 23–35
11. Sarry, J. E., Chen, S., Collum, R. P., Liang, S., Peng, M., Lang, A., Naumann, B., Dzierszinski, F., Yuan, C. X., Hippler, M., and Rea, P. A. (2007) Analysis of the vacuolar luminal proteome of *Saccharomyces cerevisiae*. *FEBS J.* **274,** 4287–4305
12. Hurlimann, H. C., Stadler-Waibel, M., Werner, T. P., and Freimoser, F. M. (2007) Pho91 is a vacuolar phosphate transporter that regulates phosphate and polyphosphate metabolism in *Saccharomyces cerevisiae*. *Mol. Biol. Cell* **18,** 4438–4445
13. Cagnac, O., Leterrier, M., Yeager, M., and Blumwald, E. (2007) Identification and characterization of Vnx1p, a novel type of vacuolar monovalent cation/H^+ antiporter of *Saccharomyces cerevisiae*. *J. Biol. Chem.* **282,** 24284–24293
14. Russnak, R., Konczal, D., and McIntire, S. L. (2001) A family of yeast proteins mediating bidirectional vacuolar amino acid transport. *J. Biol. Chem.* **276,** 23849–23857
15. Schwencke, J., and De Robichon-Szulmajster, H. (1976) The transport of S-adenosyl-L-methionine in isolated yeast vacuoles and spheroplasts. *Eur. J. Biochem.* **65,** 49–60
16. Nagy, M. (1979) Studies on purine transport and on purine content in vacuoles isolated from *Saccharomyces cerevisiae*. *Biochim. Biophys. Acta* **558,** 221–232
17. Kakinuma, Y., Masuda, N., and Igarashi, K. (1992) Proton potential-dependent polyamine transport by vacuolar membrane vesicles of *Saccharomyces cerevisiae*. *Biochim. Biophys. Acta* **1107,** 126–130
18. Hirata, T., Wada, Y., and Futai, M. (2002) Sodium and sulfate transport in yeast vacuoles. *J. Biochem.* **131,** 261–265
19. Huh, W.-K., Falvo, J. V., Gerke, L. C., Carroll, A. S., Howson, R. W., Weissman, J. S., and O'Shea, E. K. (2003) Global analysis of protein localization in budding yeast. *Nature* **425,** 686–691
20. Ghaemmaghami, S., Huh, W.-K., Bower, K., Howson, R. W., Belle, A., Dephoure, N., O'Shea, E. K., and Weissman, J. S. (2003) Global analysis of protein expression in yeast. *Nature* **425,** 737–741
21. Miller, J. P., Lo, R. S., Ben-Hur, A., Desmarais, C., Stagljar, I., Noble, W. S., and Fields, S. (2005) Large-scale identification of yeast integral membrane protein interactions. *Proc. Natl. Acad. Sci. U. S. A.* **102,** 12123–12128
22. Kumar, A., Agarwal, S., Heyman, J. A., Matson, S., Heidtman, M., Piccirillo, S., Umansky, L., Drawid, A., Jansen, R., Liu, Y., Cheung, K. H., Miller, P., Gerstein, M., Roeder, G. S., and Snyder, M. (2002) Subcellular localization of the yeast proteome. *Genes Dev.* **16,** 707–719
23. Dunkley, T. P., Watson, R., Griffin, J. L., Dupree, P., and Lilley, K. S. (2004) Localization of organelle proteins by isotope tagging (LOPIT). *Mol. Cell. Proteomics* **3,** 1128–1134
24. Dunkley, T. P., Hester, S., Shadforth, I. P., Runions, J., Weimar, T., Hanton, S. L., Griffin, J. L., Bessant, C., Brandizzi, F., Hawes, C., Watson, R. B., Dupree, P., and Lilley, K. S. (2006) Mapping the *Arabidopsis* organelle proteome. *Proc. Natl. Acad. Sci. U. S. A.* **103,** 6518–6523
25. Breitling, R., Amtmann, A., and Herzyk, P. (2004) Iterative Group Analysis (iGA): a simple tool to enhance sensitivity and facilitate interpretation of microarray experiments. *BMC Bioinformatics* **5,** 34
26. Lawson, J. E., and Douglas, M. G. (1988) Separate genes encode functionally equivalent ADP/ATP carrier proteins in *Saccharomyces cerevisiae*. Isolation and analysis of Aac2. *J. Biol. Chem.* **263,** 14812–14818
27. Kipper, J., Strambio-de-Castillia, C., Suprapto, A., Rout, M. P., and Christine Guthrie and Gerald, R. F. (2002) Isolation of nuclear envelope from *Saccharomyces cerevisiae*, in *Methods in Enzymology*, Vol. 351, pp. 394–408, Elsevier Science, USA
28. Ohsumi, Y., and Anraku, Y. (1981) Active transport of basic amino acids driven by a proton motive force in vacuolar membrane vesicles of *Saccharomyces cerevisiae*. *J. Biol. Chem.* **256,** 2079–2082
29. Keller, A., Nesvizhskii, A. I., Kolker, E., and Aebersold, R. (2002) Empirical statistical model to estimate the accuracy of peptide identifications made by MS/MS and database search. *Anal. Chem.* **74,** 5383–5392
30. Nesvizhskii, A. I., Keller, A., Kolker, E., and Aebersold, R. (2003) A statistical model for identifying proteins by tandem mass spectrometry. *Anal. Chem.* **75,** 4646–4658
31. Breitling, R., Armengaud, P., Amtmann, A., and Herzyk, P. (2004) Rank products: a simple, yet powerful, new method to detect differentially regulated genes in replicated microarray experiments. *FEBS Lett.* **573,** 83–92
32. Uttenweiler, A., Schwarz, H., Neumann, H., and Mayer, A. (2007) The vacuolar transporter chaperone (VTC) complex is required for microautophagy. *Mol. Biol. Cell* **18,** 166–175
33. Bauerle, C., Ho, M. N., Lindorfer, M. A., and Stevens, T. H. (1993) The *Saccharomyces cerevisiae* Vma6 gene encodes the 36-kDa subunit of the vacuolar H^+-ATPase membrane sector. *J. Biol. Chem.* **268,** 12749–12757
34. Wolff, A., Din, N., and Petersen, J. (1996) Vacuolar and extracellular maturation of *Saccharomyces cerevisiae* proteinase A. *Yeast* **12,** 823–832
35. Mesecke, N., Spang, A., Deponte, M., and Herrmann, J. M. (2008) A novel group of glutaredoxins in the *cis*-Golgi critical for oxidative stress resistance. *Mol. Biol. Cell* **19,** 2673–2680
36. Satyanarayana, C., Schröder-Köhne, S., Craig, E. A., Schu, P. V., and Horst, M. (2000) Cytosolic Hsp70s are involved in the transport of aminopeptidase 1 from the cytoplasm into the vacuole. *FEBS Lett.* **470,** 232–238
37. Brown, C. R., McCann, J. A., and Chiang, H.-L. (2000) The heat shock protein Ssa2p is required for import of fructose-1,6-bisphosphatase into Vid vesicles. *J. Cell Biol.* **150,** 65–76
38. Kim, S., Schilke, B., Craig, E. A., and Horwich, A. L. (1998) Folding *in vivo* of a newly translated yeast cytosolic enzyme is mediated by the SSA class of cytosolic yeast Hsp70 proteins. *Proc. Natl. Acad. Sci. U. S. A.* **95,** 12860–12865
39. Kweon, Y., Rothe, A., Conibear, E., and Stevens, T. H. (2003) Ykt6p is a multifunctional yeast r-SNARE that is required for multiple membrane transport pathways to the vacuole. *Mol. Biol. Cell* **14,** 1868–1881
40. Peplowska, K., Markgraf, D. F., Ostrowicz, C. W., Bange, G., and Ungermann, C. (2007) The CORVET tethering complex interacts with the yeast Rab5 homolog Vps21 and is involved in endo-lysosomal biogenesis. *Dev. Cell* **12,** 739–750
41. Zhang, T., and Hong, W. (2001) Ykt6 forms a SNARE complex with Syntaxin 5, GS28, and Bet1 and participates in a late stage in endoplasmic reticulum-Golgi transport. *J. Biol. Chem.* **276,** 27480–27487
42. Lewis, M. J., and Pelham, H. R. B. (2002) A new yeast endosomal SNARE related to mammalian Syntaxin 8. *Traffic* **3,** 922–929
43. MacDiarmid, C. W., Gaither, L. A., and Eide, D. (2000) Zinc transporters that regulate vacuolar zinc storage in *Saccharomyces cerevisiae*. *EMBO J.* **19,** 2845–2855
44. Grosshans, B. L., Ortiz, D., and Novick, P. (2006) Rabs and their effectors: Achieving specificity in membrane traffic. *Proc. Natl. Acad. Sci. U. S. A.* **103,** 11821–11827
45. Mayer, A., and Wickner, W. (1997) Docking of yeast vacuoles is catalyzed by the Ras-like GTPase Ypt7p after symmetric priming by Sec18p (NSF). *J. Cell Biol.* **136,** 307–317
46. Jacinto, E., and Lorberg, A. (2008) TOR regulation of AGC kinases in yeast and mammals. *Biochem. J.* **410,** 19–37
47. Chen, E. J., and Kaiser, C. A. (2003) Lst8 negatively regulates amino acid biosynthesis as a component of the TOR pathway. *J. Cell Biol.* **161,** 333–347
48. Aronova, S., Wedaman, K., Anderson, S., Yates, J., III, and Powers, T. (2007) Probing the membrane environment of the TOR kinases reveals functional interactions between TORC1, actin, and membrane trafficking in *Saccharomyces cerevisiae*. *Mol. Biol. Cell* **18,** 2779–2794
49. Beck, T., Schmidt, A., and Hall, M. N. (1999) Starvation induces vacuolar targeting and degradation of the tryptophan permease in yeast. *J. Cell Biol.* **146,** 1227–1238
50. Kunz, J., Schneider, U., Howald, I., Schmidt, A., and Hall, M. N. (2000) Heat repeats mediate plasma membrane localization of TOR2p in yeast. *J. Biol. Chem.* **275,** 37011–37020

51. Reinders, J., Zahedi, R. P., Pfanner, N., Meisinger, C., and Sickmann, A. (2006) Toward the complete yeast mitochondrial proteome: multidimensional separation techniques for mitochondrial proteomics. *J. Proteome Res.* **5,** 1543–1554
52. Cardenas, M. E., and Heitman, J. (1995) FKBP12-rapamycin target TOR2 is a vacuolar protein with an associated phosphatidylinositol-4 kinase activity. *EMBO J.* **14,** 5892–5907
53. Zhang, S., Ren, J., Li, H., Zhang, Q., Armstrong, J. S., Munn, A. L., and Yang, H. (2004) Ncr1p, the yeast ortholog of mammalian Niemann Pick C1 protein, is dispensable for endocytic transport. *Traffic* **5,** 1017–1030
54. Berger, A. C., Salazar, G., Styers, M. L., Newell-Litwa, K. A., Werner, E., Maue, R. A., Corbett, A. H., and Faundez, V. (2007) The subcellular localization of the Niemann-Pick type C proteins depends on the adaptor complex AP-3. *J. Cell Sci.* **120,** 3640–3652
55. Collins, K. M., Thorngren, N. L., Fratti, R. A., and Wickner, W. T. (2005) Sec17p and HOPS, in distinct SNARE complexes, mediate SNARE complex disruption or assembly for fusion. *EMBO J.* **24,** 1775–1786
56. Sickmann, A., Reinders, J., Wagner, Y., Joppich, C., Zahedi, R., Meyer, H. E., Schonfisch, B., Perschil, I., Chacinska, A., Guiard, B., Rehling, P., Pfanner, N., and Meisinger, C. (2003) The proteome of *Saccharomyces cerevisiae* mitochondria. *Proc. Natl. Acad. Sci. U. S. A.* **100,** 13207–13212
57. Zahedi, R. P., Sickmann, A., Boehm, A. M., Winkler, C., Zufall, N., Schonfisch, B., Guiard, B., Pfanner, N., and Meisinger, C. (2006) Proteomic analysis of the yeast mitochondrial outer membrane reveals accumulation of a subclass of preproteins. *Mol. Biol. Cell* **17,** 1436–1450
58. Wang, L., Seeley, E. S., Wickner, W., and Merz, A. J. (2002) Vacuole fusion at a ring of vertex docking sites leaves membrane fragments within the organelle. *Cell* **108,** 357–369
59. Wichmann, H., Hengst, L., and Gallwitz, D. (1992) Endocytosis in yeast: evidence for the involvement of a small GTP-binding protein (Ypt7p). *Cell* **71,** 1131–1142
60. Tarassov, K., Messier, V., Landry, C. R., Radinovic, S., Molina, M. M. S., Shames, I., Malitskaya, Y., Vogel, J., Bussey, H., and Michnick, S. W. (2008) An in vivo map of the yeast protein interactome. *Science* **320,** 1465–1470
61. Decker, B. L., and Wickner, W. T. (2006) Enolase activates homotypic vacuole fusion and protein transport to the vacuole in yeast. *J. Biol. Chem.* **281,** 14523–14528
62. Gary, J. D., Sato, T. K., Stefan, C. J., Bonangelino, C. J., Weisman, L. S., and Emr, S. D. (2002) Regulation of Fab1 phosphatidylinositol 3-phosphate 5-kinase pathway by Vac7 protein and Fig4, a polyphosphoinositide phosphatase family member. *Mol. Biol. Cell* **13,** 1238–1251
63. Bonangelino, C. J., Catlett, N. L., and Weisman, L. S. (1997) Vac7p, a novel vacuolar protein, is required for normal vacuole inheritance and morphology. *Mol. Cell. Biol.* **17,** 6847–6858
64. Cooke, F. T., Dove, S. K., McEwen, R. K., Painter, G., Holmes, A. B., Hall, M. N., Michell, R. H., and Parker, P. J. (1998) The stress-activated phosphatidylinositol 3-phosphate 5-kinase Fab1p is essential for vacuole function in *S. cerevisiae. Curr. Biol.* **8,** 1219–1222
65. Gary, J. D., Wurmser, A. E., Bonangelino, C. J., Weisman, L. S., and Emr, S. D. (1998) Fab1p is essential for Ptdins(3)p 5-kinase activity and the maintenance of vacuolar size and membrane homeostasis. *J. Cell Biol.* **143,** 65–79
66. Vickers, M. F., Yao, S. Y. M., Baldwin, S. A., Young, J. D., and Cass, C. E. (2000) Nucleoside transporter proteins of Saccharomyces cerevisiae. Demonstration of a transporter (Fui1) with high uridine selectivity in plasma membranes and a transporter (Fun26) with broad nucleoside selectivity in intracellular membranes. *J. Biol. Chem.* **275,** 25931–25938
67. Springael, J.-Y., and Andre, B. (1998) Nitrogen-regulated ubiquitination of the Gap1 permease of *Saccharomyces cerevisiae. Mol. Biol. Cell* **9,** 1253–1263
68. Chuang, J. S., and Schekman, R. W. (1996) Differential trafficking and timed localization of two chitin synthase proteins, Chs2p and Chs3p. *J. Cell Biol.* **135,** 597–610; Correction (1996) *J. Cell Biol.* **135,** 1925
69. Albertsen, M., Bellahn, I., Kramer, R., and Waffenschmidt, S. (2003) Localization and function of the yeast multidrug transporter Tpo1p. *J. Biol. Chem.* **278,** 12820–12825
70. Beeler, T., Fu, D., Rivera, J., Monaghan, E., Gable, K., and Dunn, T. (1997) Sur1 (Csg1/Bcl21), a gene necessary for growth of *Saccharomyces cerevisiae* in the presence of high Ca^{2+} concentrations at 37 °C, is required for mannosylation of inositolphosphorylceramide. *Mol. Gen. Genet.* **255,** 570–579